1-1-2012

Uracil accumulation in folate depleted mouse embryonic fibroblasts

Eneida Doko
Wayne State University,

URACIL ACCUMULATION IN FOLATE DEPLETED MOUSE EMBRYONIC FIBROBLASTS

by

ENEIDA DOKO

THESIS

Submitted to the Graduate School

of Wayne State University,

Detroit, Michigan

in partial fulfillment of the requirements

for the degree of

MASTER OF SCIENCE

2012

MAJOR: NUTRITION & FOOD SCIENCE

Approved by:

_____

Advisor Date

DEDICATION

I dedicate this thesis and all of the hard work behind it to my family and friends. I am very grateful to have a family that is always supportive, helpful, loving, and by my side during the good and bad times throughout my life. Thank you Begator, Shpresa, Ernada, and Leo Doko for everything. My friends have also been an amazing support throughout this experience. If it were not for them, I would not been able to get back on my feet during those hard times in my life. Thank you Saddig Kaid, Moby A. and Amanda Smith.

ACKNOWLEDGMENTS

I would like to acknowledge and give my most sincere gratitude to my amazing advisor, Dr. Diane Cabelof. Through her guidance and support, I have grown both as a student and a person, and I leave with the confidence that I will be able to successfully accomplish my career goals. I would also like to thank my committee members, Dr. Heydari and Dr. Yifan Zhang. They were both very helpful and caring throughout the entire process, and their generous offerings of expertise helped me create my best work. Lastly, I would also like to thank my lab members Honghzi Ma, Kirk Simon, and Aqila Ahmed for their help and contributions during my research in the lab. Working with such great people in the lab was an incredible experience. Throughout my tenure at Wayne State, I learned a lot and pushed myself beyond my limits, and I have also made many great friendships that I will always cherish. Thanks again to all of you.

TABLE OF CONTENTS

LIST OF TABLES

LIST OF FIGURES

INTRODUCTION

The pharmaceutical business in today's society is a billion-dollar industry due to the mindset that each health problem should be accompanied with a pharmaceutical resolution. Recent scientific research supports the view that nutrition plays a pivotal role in preventing, delaying, or regressing the development and progression of different cancers and other human related diseases. Most importantly, current health issues are influenced by our nutrition and diet. The possibility of an individual being at risk for cardiovascular disease, cancer and other chronic diseases depends on what types of food we consume on a daily basis.

Folate has emerged as a major determinant in the pathogenesis of several malignancies, most convincing relates to colon cancer [1]. Human studies have shown that folate deficiency (serum folate less than 3 ng/ml or erythrocyte folate below 140 ng/ml) [2] is associated with cancers of the brain, breast, pancreas, lung, cervical, liver, and esophagus [3]. Other common diseases and developing anomalies as a result of folate deficiency include cardiovascular disease, intestinal cancers, Alzheimer's disease, and neural tube defects (NTD's) [9] as listed in Table 1 by Barry Shane, Ph.D. Folate, a methyl group ($-CH_3$) carrier involved in *de novo* nucleotide syntesis, plays a significant role in several different body functions and biosynthetic pathway reactions. Some of these biochemical processes include DNA metabolism, DNA repair, DNA methylation, and cellular growth. Most importantly, folate deficiency has been shown to increase uracil misincorporation in DNA and therefore induce DNA damage repaired by the base excision repair (BER) pathway [1-3].

Metabolic Disruption	Biochemical Markers	Clinical Associations
S-adenosymethionine (MTHFR, MS, B12 Deficiency)	Hypomethylation DNA Elevated homocysteine Reduced mythlation	Cancer CVD Demyelination NTDs
Thymidylate	Increased uracil in DNA Decreased DNA synthesis & Reduced cell division	Cancer NTDs Anemia
Purines (A, G)	Increased uracil in DNA Decreased DNA synthesis & Reduced cell division	Anemia

Table 1: Adverse health affects as a result of impaired folate status or metabolism.

Folate, derived from the Latin word “folium” meaning leaf, is a water-soluble B vitamin that occurs naturally in foods [4]. Folic acid, also known as pteroylmono-glutamic acid (PGA), is the synthetic and completely oxidized form of folate that is found in supplements and used as an additive in fortified foods, typically in grains, breads, and ready-to-eat breakfast cereal [5]. Natural sources of folate include leafy green vegetables (especially spinach, peas, asparagus, and turnip greens); fruits such as strawberries, oranges, cantaloupes, and other melons; meats (essentially liver and other liver prodcuts) and legumes. Fruits and vegetables supply more than one-third of folate whereas grain products provide approximately one-fifth of folate in the American diet [6]. In 1996, the Food and Drug Administration (FDA) required the addition of folic acid in grain products such pastas, cereals, breads, flours, and rice in order to decrease the risk of birth defects in newborns[7,8]. Hence, cereals and grains have become a significant contributor of folic acid to the American diet since such products are most commonly consumed by today’s Western diet.

Folic acid consists of a pterin ring that is attached to p-aminobenzoic acid (PABA) and connected to one or more residues of glutamate (Fig. 1) [10]. Since humans cannot produce PABA and conjugate the first glutamate, they are incapable of synthesizing folate endogenously. Folate in natural foods and tissues exists in the form of polyglutamates in order to keep the folate within the cells. However, in urine and plasma, folate is found in the monoglutamate form that can easily be transported across cell membranes. Polyglutamate, in the lumen of the small intestine, is converted by different enzymes to monoglutamate and then absorbed in the proximal jejunum through active and passive transport [10].

Folate within the plasma exists as the inactive metabolite of 5-methylet-etrahydrofolate (5-methyl THF). Once 5-methyl THF enters the cell through several different folate transporters

with differing affinities and mechanisms, it is demethylated by the methyl cofactor B-12 (cobalamin) to the active form of tetrahydrofolate (THF) that is responsible for the transferring of one carbon unit in the *de novo* synthesis of nucleotides [11]. With the absence of vitamin B-12, the inactive form of 5-methyl THF cannot be converted to the active form of THF for further metabolic pathways. This is known as the folate trap (Figure 2). However, increase in folate supplements can bypass the folate trap.

Figure 1: Components of folic acid [10].

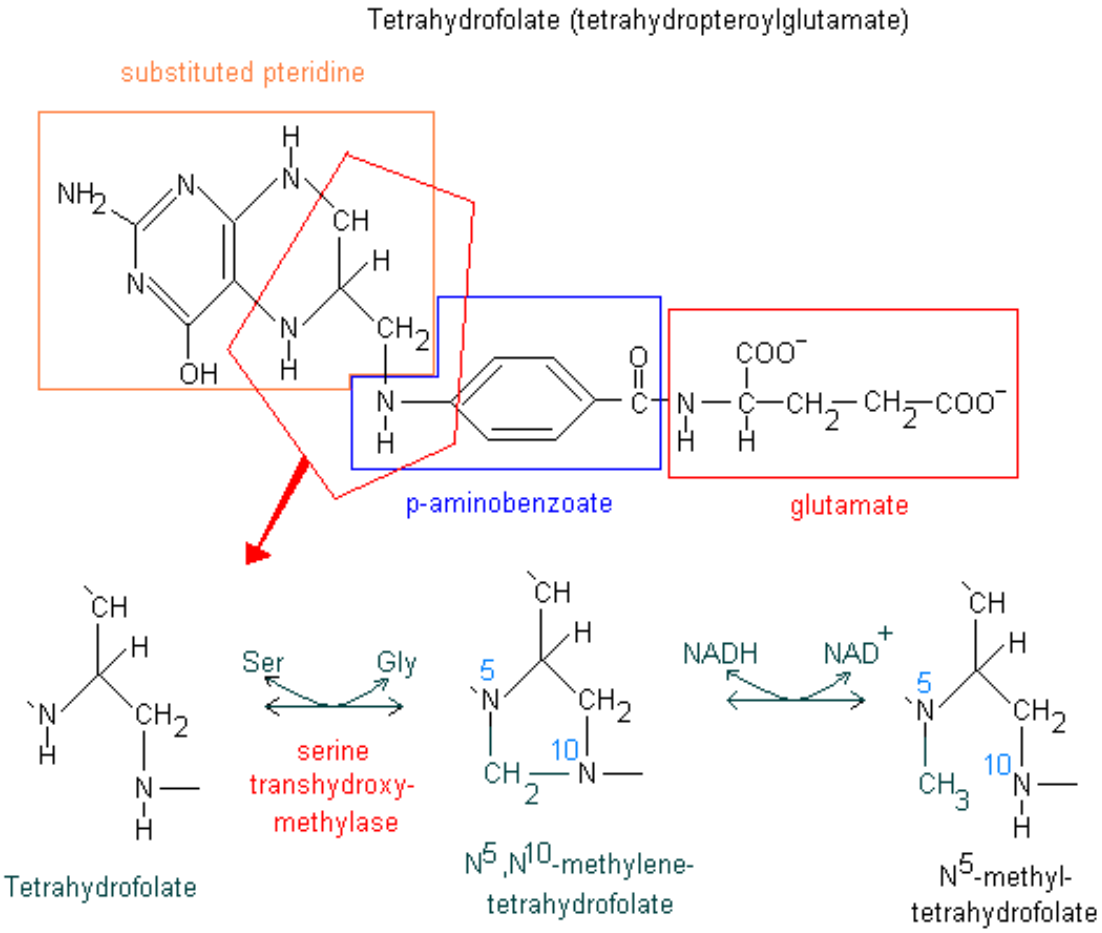

Figure 2: Different folate pathways including "Folate Trap" [19].

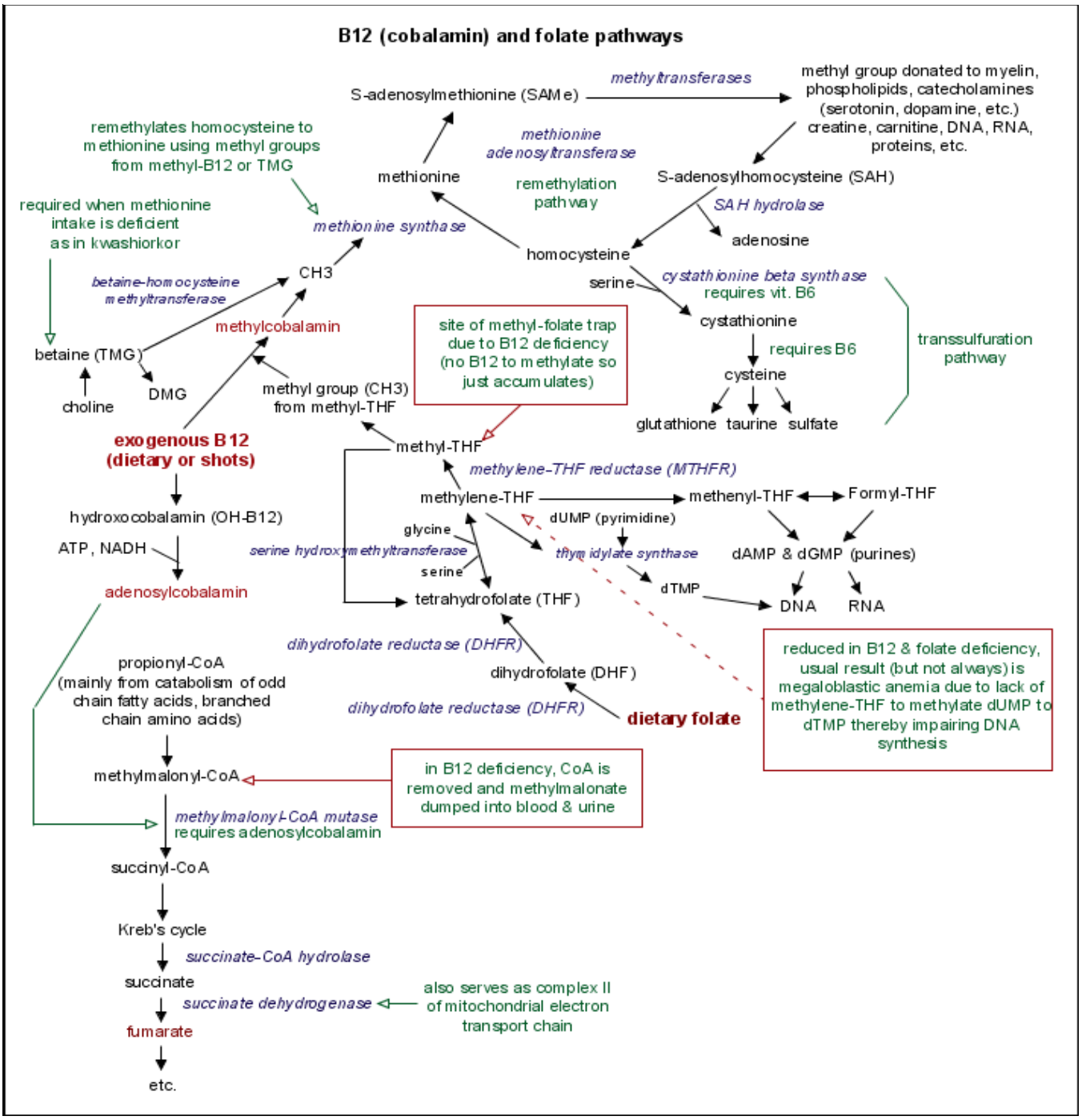

Folic acid is the active form of tetrahydrofolic acid (THFA) and is considered more stable than dietary folate. THFA is generated by the 2-step reduction of folate using the enzyme dihydrofolate reductase. Dietary folate is approximately 50% bioavailable whereas folic acid is about 85% bioavailable when consumed with food [12]. The bioavailability of folate depends on the polyglutamate chain in which most of the dietary folate is attached. The bioavailability of dietary folate is reduced by as much as 25-35% once the polyglutamate chain has been removed by the intestinal conjugase [12]. Hence, food fortifications can significantly increase the amount of folic acid in the diet. For instance, at least 25% of the Recommended Dietary Allowance (RDA) for folate is generally found in ready-to-eat fortified breakfast cereals [6-8]. The USDA created the Dietary Reference Intakes (DRIs) for recommended intake of folate [13]. Three singificant reference of values are found in the DRIs that include the Tolerable Upper Intake Levels (UL), Recommended Deitary Allowances (RDA), and Adequate Intakes (AI). The Dietary Folate Equivalent (DFE) is a term used to express the RDAs for folate in micrograms (µg). DFE was created in order to account for the difference of natural folate absorption and folic acid bioavailability. Table 2 lists the RDAs for folate intake for children and adults, expressed in micrograms (µg) of DEF among children and adults. One DEF is equivalent to 1 µg of food folate which equals to 0.6 µg of folic acid from supplements and fotified foods. As indicated in the table, pregnant women have a higher RDA for folate in order to prevent the incidence of birth defects such as NTD's (neural tube defects) and other potential malformations in their babies such as cleft palate during pregnancy [8,10].

Table 2: Recommended Dietary Allowances for Folate.

Folate RDAs Across the Life Cycle	
	µg/day
Infants (AI)	**65 - 80**
Children	**150 – 300**
Adolescents and Adults	**400**
Elderly Subjects	**400**
Pregnant Women	**600**
Lactating Women	**500**

Some people may also require a higher intake folic acid especially during medical conditions that either increase the need for folate or decrease folate absorption. For instance, individuals with alcohol abuse, kidney dialysis, malabsorption, sickle cell disease, celiac disease and liver disease require much more folic acid than recommended by the RDA [5]. Medications used to treat epilepsy, type II diabetes, asthma, lupus, rheumatoid arthritis, inflammatory bowel disease, and psoriasis affects folate metabolism and therefore may cause folate deficiency. Folate, in its reduced form THF, has the principal biochemical function of acting as a co-factor conveyor of one-carbon units at different states of oxidation and participating in one-carbon transfer (Fig. 3) [14]. Certain derivatives of THF are significant factors in different metabolic pathways. 5-methyl THF, 5,10-methylene THF, and 10-formyl are three of the one carbon substituted derivatives that play a huge role in the synthesis of methionine, thymidylate, and purine respectively [14].

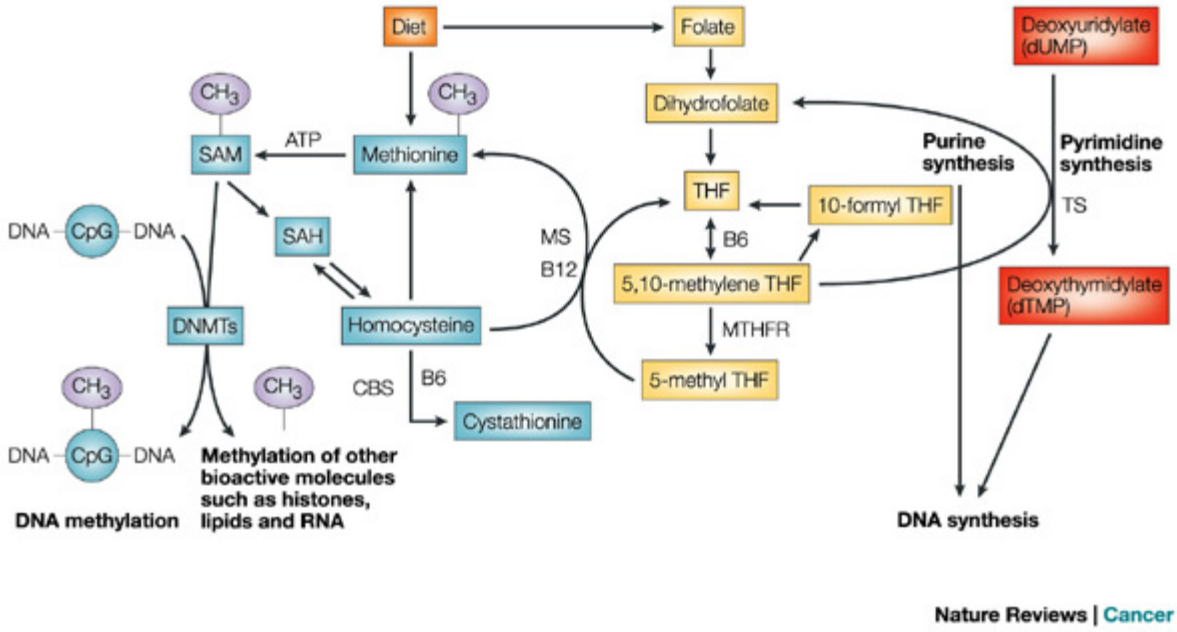

Figure 3: Metabolic pathways involving different derivatives of folate [14].

The predominant circulating form of folate (5'-methyl-THF) is an essential cofactor in the conversion of homocysteine to methionine [11,14,15]. Once methionine reacts with ATP, it is then converted to its active form S-adenosylmethionine (SAM), the methyl donor (-CH3) in several different biosynthetic reactions such as cytosine methylation in DNA. Cytosine methylation, a nonspontaneous process, is a non-mutational epigenetic change that occurs within the cytosine-guanine dinucleotide CpG sequence, specifically at the 5' carbon of the cytosine. It is hereditable and affects the hereditary information specified by the DNA base sequence. Complex enzymes such as DNA methyltrasferases (DNMTs) that catalyze the synthesis of 5' methylcytosine (the 'fifth' DNA base) are important for accurately copying the DNA-methylation sequence in normal cells during replication [14]. DNA methylation plays an important role in the inhibition of transcription initiation (chromatin remodeling) and stability of the genome.

During folate deficiency, SAM becomes depleted, reducing the methylation of cytosine in DNA. Such hypomethylation may upregulate the expression of proto-oncogenes and eventually induce cancer as shown in Figure 7 [14-16]. Studies have shown that specific human genes such as proto-oncogenes and growth hormones from lung and colon tumors are substantially hypomethylated (less methylated) compared to genes from normal adjacent tissues [16]. Since folate has a fundamental role in the methylation of cytosine, it therefore has the ability of regulating gene expression. Rate of transcription is reduced or inhibited during the methylation of genes at specific locations in DNA. Gene expression and function is controlled by site-specific DNA methylation. Malignant transformation may increase as a result of alterations or disruptions in either global or site-specific methylation [16].

Folate is also required for transferring one-carbon units in the *de novo* synthesis of the essential pyrimidine nucleoside, thymidine as shown in Fig. 4 [11,14-16]. Thymidylate is

produced by the *de novo* nucleotide synthesis that requires folate and the salvage pathway that does not require folate. 5,10-methylene- tetrahydrofolate, which is reduced to 5-methyl THF by methylene tetrahydrofolate reductase (MTHFR), is the methyl donor for the conversion of dUMP (dexoyuridine monophosphate or deoxyuridylate) to dTMP (deoxythymidine monophosphate or deoxythymidylate) by thymidylate synthase (TS) (Fig. 4). The conversion of dUMP to dTMP is an irreversible rate-limiting step. If levels of folate are low, dUMP accumulates resulting in uracil misincorporation into DNA in place of thymine. Decrease in folate leads to a decrease in the synthesis of thymidylate, increasing the cellular dUMP/dTMP ratio and DNA polymerase-mediated dUTP misincorporation into DNA. Moreover, the *de novo* nucleotide synthesis of deoxythymidylate is important for the fidelity of the DNA message. Once uracil is removed from the DNA strand by Uracil-DNA glycosylase, transient single strand breaks called nicks are generated. Such nicks could lead to double stranded breaks that are less likely to be repaired and increasingly hazardous if two opposite nicks are formed. A continuous repeat of uracil misincorporation and repair due to folate deficiency may occur in a 'catastrophic' or 'futile' repair cycle [16], inducing breakage of the DNA molecule, malignant transformation, and chromosomal damage (Fig. 5). Several studies have shown that the misincorporation and removal of uracil in DNA cause chromosomal breaks in tumor cells that were not treated with folate [2,14-17].

Figure 4: Thymidylate synthase reaction.

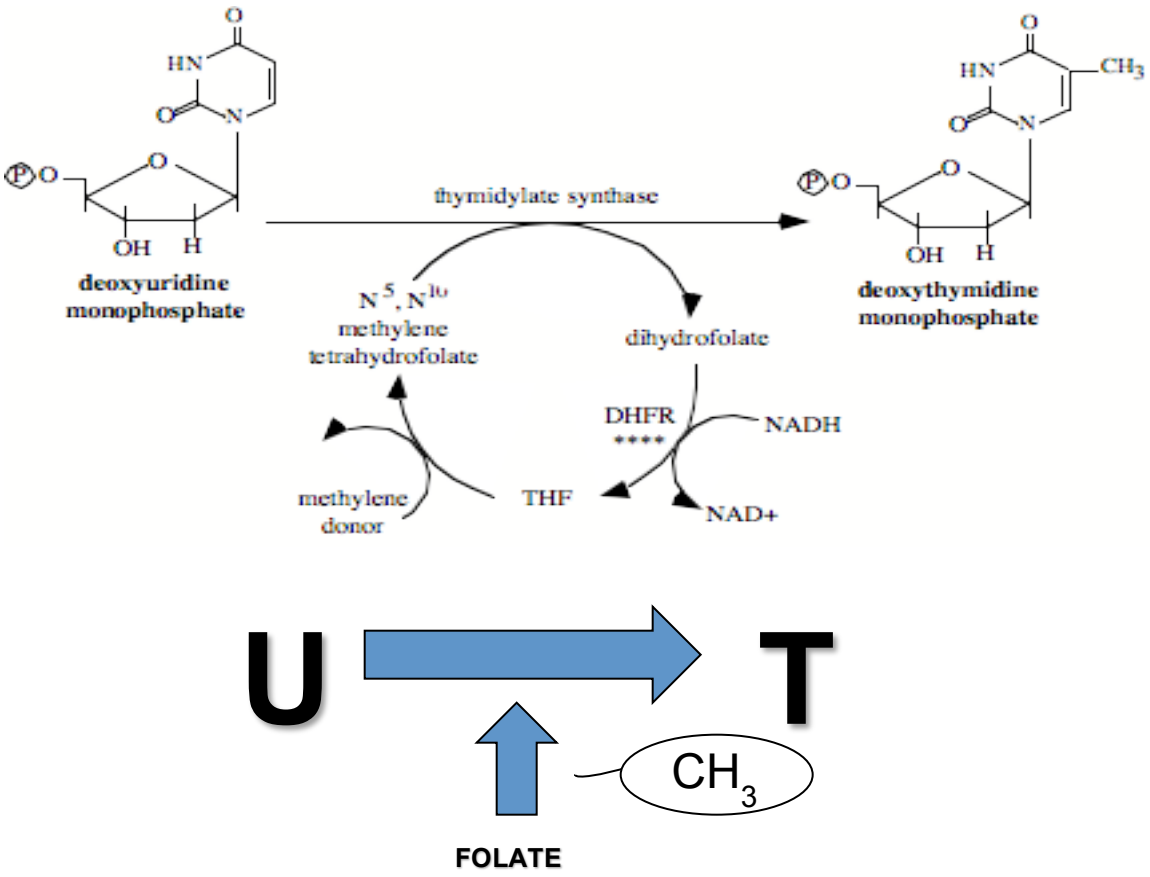

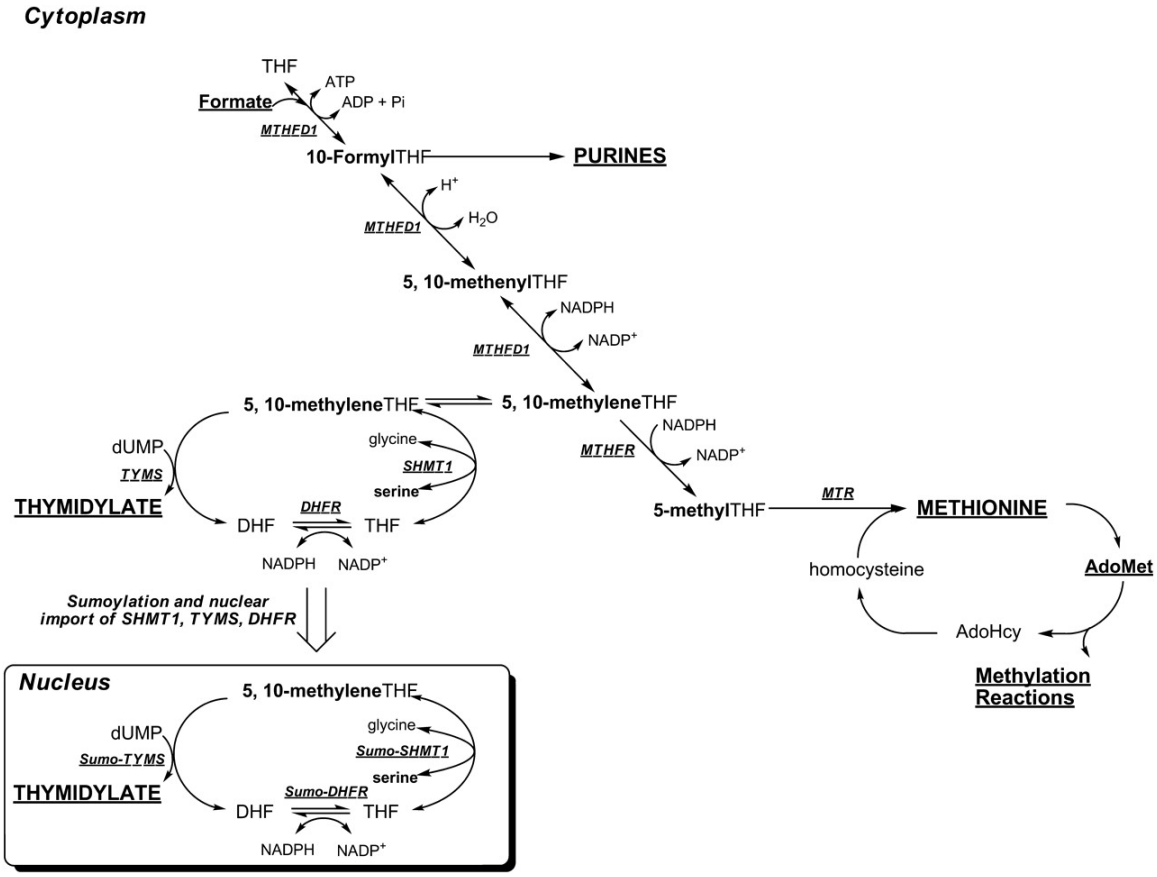

Figure 5: Folate-mediated 1-carbon metabolism [14].

Folate deficiency has been shown to induce uracil misincorporation by a virtue of thymidylate depletion. Majority of uracil lesion in DNA occur from the incorporation of dUMP instead of dTMP during replication, generating U: A pairs. Hydrolytic cytosine deamination may also enhance the amount of incorporated uracil in DNA, creating mutagenic U: G mismatches. Base excision repair (BER) is the sequential pathway initiated by a uracil-DNA glycosylase (UDG) to repair misincorporated uracil [3]. Base excision repair pathway is also responsible for repairing endogenous DNA damage and damages as a result of alkylation and oxidative stress. BER repairs small, non-helix distorting base lesions through either the short-patch or long-patch BER pathway. Short-patch BER involves the replacement of only one nucleotide at a time whereas the long-patch BER replaces 2-13 nucleotides (3,18).

Figure 6: BER pathway.

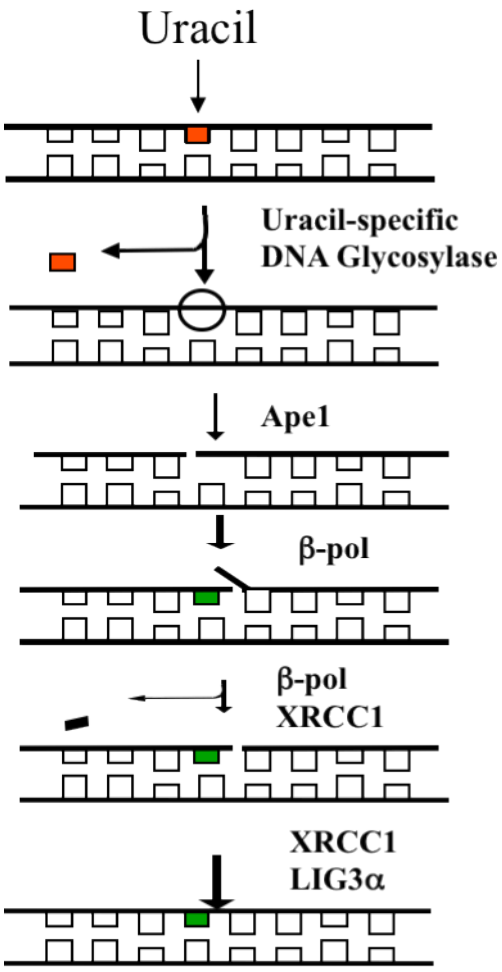

In the BER pathway, UDG cleaves the N-glycosidic bond between the base and deoxyribose, creating a transient abasic site (AP-site). AP-endonuclease 1 (APE1) then recognizes and cleaves the DNA 5' at the AP-site. APE1 leads to the formation of a strand break with a 3'-hydroxyl group and an abnormal 5'-abasic terminus. From then on, the BER may follow either the short-patch or long-patch route. During the short-patch pathway, BER continues with the DNA polymerase B (B-pol) that removes the 5'-abasic residue and fills in the single nucleotide gap. Then, a complex of XRCC1 and Ligase III seals the nick. The short patch, which accounts for 70-90% of the BER pathway, generally repairs uracil misincorporation in DNA due to folate deficiency [18]. Studies have shown that the initiation of BER is induced due to folate deficiency by upregulating uracil-DNA glycosylase (UDG) expression and activity while inhibiting the upregulation of the rate determining enzyme β-pol (DNA polymerase) of the BER pathway [3,18].

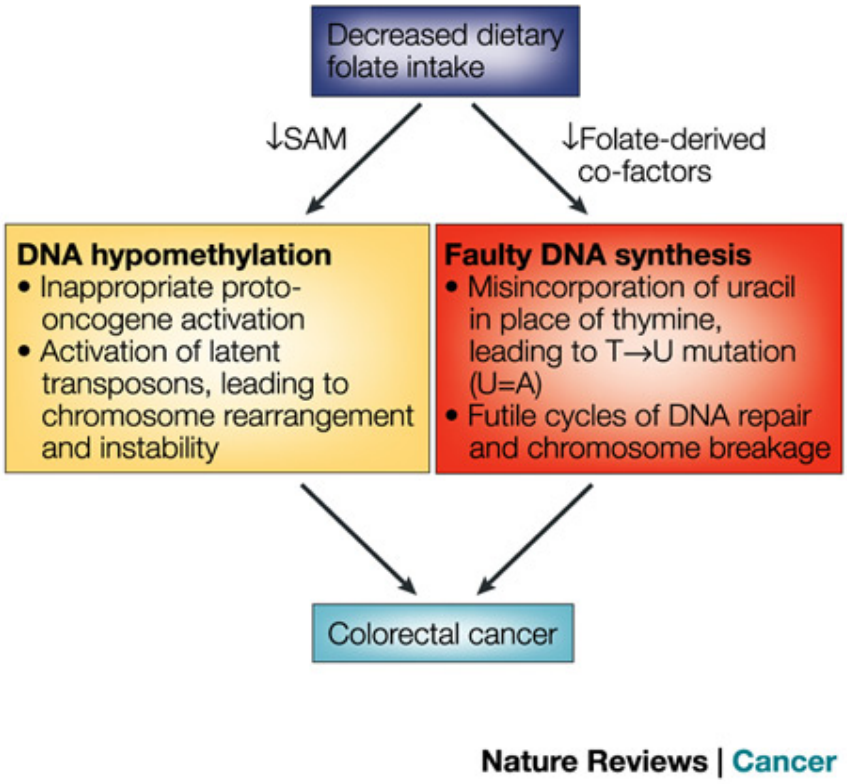

Figure 7: Affect of dietary folate on DNA methylation and synthesis [14].

The objective of this research is to determine the effect of cell growth in response to folate deficiency. Most importantly, to determine the impact of folate depletion on uracil accumulation, BER activity and UDG activity in wild type and $UNG^{-/-}$ knockout mouse embryonic fibroblasts (MEFs). Previous studies have shown that folate deficiency results in uracil misincorporation in DNA and therefore increasing genomic instability. Uracil is excised from DNA by the uracil DNA glycosylase (UDG) during the BER pathway. According to experimental evidence, the capacity of BER pathway is also impacted by folate deficiency. We therefore hypothesize that **folate depletion will impact BER response through uracil accumulation in genotype-dependent manner**. Our hypothesis will be investigated by the following aims:

Specific Aim 1: to determine the effect of genotype on cell growth in response to folate depletion.

Specific Aim 2: to determine the effect of genotype on uracil accumulation in response to folate depletion.

Specific Aim 3: to determine the effect of genotype on BER in response to folate depletion.

MATERIALS AND METHODS

Tissue Cultures:

Transformed SV40 T-antigen mouse embryonic fibroblasts (MEFs) were derived from the embryos ($ung^{+/+}$ and $ung^{-/-}$) of the ung moused developed by Endres et al. [22]. These cells were grown in either folate added standard DMEM (GIBCO BRL, Grand Island, NY, USA) containing 4.5g/L glucose, 4mg/L folic acid, glutamax, glutamine, 10% un-dialyzed fetal bovine serum or customized folate-free DMEM (GIBCO BRL) media supplemented with 10% dialyzed fetal bovine serum, glutamax and glutamine. Each of the growth media was supplemented with 1% penicillin-streptomycin and both $UNG^{+/+}$ and $UNG^{-/-}$ cells were incubated at 37°C in 10% $C0_2$. Folate-free media was also supplemented with thymidine and adenosine at different concentrations in order for the cells to survive. The percentage of T/A was achieved over time through a stepwise reduction, 1X being the starting concentration. The mouse embryonic fibroblast cells were passaged three times for each T/A concentration until 0% T/A was achieved. Before each passage, the cells were grown until they became 75% confluent. The cells were passaged the same way as they were passaged for the doubling times.

Harvesting Cells:

The flasks of cells were first visualized under the microscope to determine if the cells were 75% confluent. The old media from the cells was removed and the flasks were washed with 5 ml of pre-warmed 1X PBS-EDTA. Once the 1X PBS-EDTA was removed, 2 ml of trypsin was added. The flasks were then incubated for approximately 2-3 minutes at 37°C in order to detach the cells from the bottom of the flask. The cells were again viewed under the microscope to ensure that the cells were lifted off the flask. To stop the trypsin from working, 4-5 ml of complete growth media was added. Using a serological pipette, the cells were pipette up and

down several times for the cells to separate from each other. The cells along with the added complete media were transferred into a 15 ml conical tube for washing. The cells were centrifuged for 5 minutes at 1300 rpm at 4°C. The media was carefully removed without disturbing the white visible pellet on the bottom of the conical tube and 5 ml of 1X PBS was added to the pellet. The cells were again centrifuged at 1300 rpm for 5 minutes at 4°C and the 1X PBS was carefully removed without removing the pellet. A little bit of PBS was left behind covering the pellet in order for the pellet not to dry out. The pellet (cells) were then stored at -80°C to freeze for the next step in DNA isolation.

DNA Isolation:

Once the cells were harvested, the genomic DNA was isolated using the QIAGEN gravity tip columns (Valencia, CA). The cells were removed from -80°C and thawed on ice. The cells were washed twice in PBS and resuspended in 0.5 ml cold PBS (4°C). Since our cell culture did not exceed more than $5x10^6$ cells, 0.5 ml suspension was used to isolate the genomic DNA. One volume (0.5 ml) of ice-cold Buffer C1 and 3 volumes (1.5 ml) of ice-cold distilled water were added to the pellet along with the PBS. The tube was inverted several times to mix and incubated on ice for 10 minutes. The lysed cells were centrifuged at 4°C for 15 minutes at 1300 x g and the supernatant was discarded. Then, 0.25 ml of ice-cold Buffer C1 and 0.75 ml of ice-cold distilled water was added and vortexed. The pellet was then centrifuged again at 4°C for 15 minutes at 1300 x g. The supernatant was removed and 1 ml of Buffer G2 was added. The nuclei was completely resuspended by vortexing for 30 seconds at maximum speed. Then, 25µl of QIAGEN Proteinase K stock solution was added and incubated at 50°C for 60 minutes. Slightly before the end of the 60 minute incubation period with Proteinase K, the QIAGEN Genomic-tip 20/G were equilibrated with 2 ml of Buffer QBT and allowed to empty by gravity flow. The samples were

vortexed for 10 seconds at maximum speed and applied to the equilibrated QIAGEN Genomic-tips. The samples were allowed to enter the resin of the column tips by gravity flow. The Genomic-tips were washed 3X with 1 ml of Buffer QC. The genomic DNA was then eluted 2X with 1 ml of Buffer QF. The DNA was precipitated by adding 1.4 ml (0.7 volume) of room-temperature isopropanol to the eluted DNA. The precipitated DNA was then recovered by inverting the tube 10-20 times and spooling the DNA using a glass rod. The spooled DNA was then immediately transferred to a microcentrifuge tube containing 0.1 ml of TE buffer (pH 8.0). The DNA was then left to dissolve overnight and stored at -20°C.

Folate Microbiology Assay

Folate was measured from the UNG $^{+/+}$ and UNG $^{-/-}$ cells using the folate microbiological assay as described by Home et al [25]. This widely used microbiological assay measures folic acid derivatives in serum as well as other biological samples [25]. The folinic acid (calcium salt) [(6-ambo)-5-HCO-H4PteGlu] was prepared in water at a concentration of 6 mM (6×10^6 fmol/µ) and diluted to 6×10^3 fmol/µl, which was then diluted to 60 fmol/ µl and eventually to a final dilution of 2b fmol/µl (working solution). The single strength folic acid casei medium was prepared by dissolving 9.4 gram of the powder folic acid casei medium and 50 mg of sodium ascorbate (Vitamin C) into 100 ml of diH_2O. The mixture was then filtered through a 0.22-µm sterile syringe filter. The working buffer was prepared by dissolving 3.2 gram of sodium ascorbate into 19 ml of diH_2O and adding 1 ml potassium phosphate buffer (1mol/l, pH 6.1). The mixture was then sterilized through a 0.22-µm sterile syringe filter. Lastly, the *L. casei* inoculum was prepared. One vial of lyophilized *Lactobacillus casei*, stored at -80^{o}C when first received, was suspended in 1 ml of the medium to grow overnight at 37^{o}C. From this inoculum, 0.25 ml was added to the remaining 199 mL of medium and incubated for approximately 18 hours at

35°C. The mixture was then cooled down in an ice bath. An equal volume of cold (4°C) sterile glycerol (800ml/L) was added to the mixture. From the mixture, 2-ml aliquots were prepared and stored at -80°C.

Once the *L. casei* inoculum was incubated overnight at 37°C, the OD was measured and diluted to an OD value of 0.5 (the standard OD value of the *L. casei* inoculum). The microtiter plate was then set up as shown in Table 3a. A multiple pipette was used to add the working buffer mixture (8 µl/sample) and media (150 µl/sample) along with either autoclaved or sterile water. As shown in Table 3a, 2 fmol/ µl of folate with the corresponding volume was added to each designated well on the plate. Due to folate being light sensitive, the lights were turned off during the procedures of this assay. Using a multiple pipette, 20 µl of *Lactobacillus casei* (OD=0.05) was added to the standards and samples for the exception of one blank. Autoclaved or sterile water was added around the well of the microtiter plate to create enough humidity whereas parafilm was used to cover the plate in order to keep the humidity within the microtiter plate. The plate was also covered with oil film to prevent the degrading of folate from light. The plate was incubated overnight at 37°C for approximately 18 hours. Before the plate was read at an absorbance of approximately 570-635 using a Dynatech Model MR600 reader, the pellet of the bacteria was resuspended using a pipette.

Doubling Times:

The MEF cells, using proper sterile techniques, were examined daily under a light microscope, observing the morphology, density of the cells, and color of the media. Once the cells became 75% confluent, the 10 mm petri dishes containing the cells were carefully removed from the incubator. Under the laminar flow hood, the media was carefully discarded and the plates were washed in 5 ml pre-warmed 1X PBS-EDTA. Following the removal of 1X PBS-

EDTA, 2 ml of the pre-warmed dissociation reagent, trypsin, was gently added and left to incubate for 3-5 minutes so the cells could completely detach from the flasks. The cells were then observed under the microscope for detachment and gently rocked or tapped against a nearby object in order to completely lift the cells from the flasks and 3 ml of pre-warmed complete growth media was added. Once a single cell suspension was achieved, the cells were transferred into a 15-ml conical tube. Trypan blue (10µl), which is rejected by live cells but accumulates in dead cells, was transferred into a 1.5 ml eppendorf tube along with 20µl of cells and counted in the TC 10 Automated Cell counter. The total number of cells/ml was then calculated and used to determine the amount of cells to plate for the next passage.

Calculations:

Live conc. cell count x 2 (1:2 trypan blue dilution) = # of cells/ml
EX: 2.56 x 10^5cells/ml x 2 = 512,000 cells/ml

Must be consistent throughout each passage when performing doubling time

$$\frac{\text{\# of cells to be plated}}{\text{\# of cells/ml}} = \text{amt of cells in ml or µl to be plated for next doubling time passage}$$

EX: $\frac{250,00 \text{ cells}}{512,000 \text{ cells/ml}}$ = 0.4822 ml or 488 µl of cells to be plate in order to grow 250,000 cells in the next passage

Total # of cells/flask = (# of cells/ml) x 2 (trypan blue dilution) x total volume

UDG-ASB (Uracil Assay):

Uracil was measured as described by Cabelof et al. [24] Once the DNA was isolated using the QIAGEN gravity tip columns, the DNA concentration was measured and quantified using the Thermo Scientific NanoDropTM 1000 Spectrophotometer. From the spectrophotometer readings, 4µg of total DNA was taken from each group sample and brought up to 100µl in TE buffer (pH 7.6). The 4µg of DNA was then blocked in a freshly made 2X tris/methoxyamine buffer (final concentration: 100mM methoxyamine (Sigma-Aldrich, St. Louis, MO) and 50mM Tris-HCl) for 2 hours at 37°C while covered completely with aluminum foil due to the methoxyamine being light sensitive. DNA was then precipitated with 10% volume of 2 M NaCl and .4µg/µl of glycogen was added followed by 1 volume of isopropanol. The DNA was then inverted or mixed gently, held at -70°C for 15 minutes and then centrifuged at 14000 x g for 15 minutes at 4°C. The supernatant was then removed and the visible white pellet of DNA was left to air dry at room temperature for 2 minutes. DNA was then washed with 4 volumes of 70% ice cold ethanol, centrifuged again at 14000 x g for 15 minutes at 4°C. Once the ethanol was removed, the white pellet of DNA was left to air dry again at room temperature for 5 minutes. The dry pellet of DNA was resuspended in TE buffer, pH 7.6. DNA was then treated with 0.4 units of Uracil DNA Glycosylase (UDG) (New England Biolabs, Ipswich, MA) for 15 minutes at 37°C heat block. DNA was immediately precipitated again as previously described (NaCl, 0.8µg/µl glycogen, isopropanol), washed with ethanol and resuspended in TE buffer, pH 7.6. DNA was then probed with 2 mM aldehydic reactive probe (ARP) (Dojindo Molecular Technology, Gaithersburg, MD) and incubated in 37°C heat block for 15 minutes. DNA was again precipitated as previously described (NaCl/0.4µg/µl glycogen, isopropanol). However, the DNA pellet this time was washed twice with ethanol to completely remove any left over probe

residues before it was re-suspended one last time in TE buffer (pH 8.0) and quantified.

From the probed DNA quantifications, the volume of DNA required for 0.5µg DNA was calculated and brought to a volume of 220µl with TE buffer (pH 7.6). DNA was then heat denatured at 100°C for 10 minutes in a heat block. Before the DNA samples were removed from the heat block, an equal volume of 2 M ammonium acetate was added to the DNA samples (prevent re-annealing of the DNA when cooling down), immediately vortexed well and chilled on ice. A nitrocellulose membrane (Schleicher and Schuell, Dassel, Germany) was pre-wet in deionized water and washed for 10 minutes in 1 mM ammonium acetate before it was placed on the slot blot apparatus. While the nitrocellulose membrane was being washed, the slot blot apparatus was properly attached to the vacuum. Before loading the samples, the clamp on the slot blot apparatus was tightened while maintaining the vacuum OFF, 220µl of 1 mM ammonium acetate was added to each individual well of the slot bot and then vacuumed. The entire genomic DNA/ammonium acetate was then applied gently to each slot well while keeping the vacuum OFF. Before the vacuum was applied, the samples from each group were pipetted up and down several times in each well to eliminate air bubbles, therefore, to ensure much sharper and tighter bands on the nitrocellulose membrane. Once all the samples were loaded and the vacuum was applied, each slot was washed with 200µl of 1 M ammonium acetate and vacuumed again. The nitrocellulose membrane was then washed in pre-warmed (37°C) 5 X SSC (saline sodium citrate) solution, incubated for 15 minutes at 37°C at 50 rpm while being completely covered in aluminum foil, and baked on a blotting paper under vacuum at 80°C for 30 min. The dried nitrocellulose membrane was then incubated in a 40 ml prehybridization buffer (1 mM Tris, pH7.5, 5 M NaCl, 0.5 mM EDTA, 0.5% (w/v) casein, 0.25% (w/v) bovine serum albumin, 0.1% (w/v) Tween 20) for 30 minutes at room temperature. The nitrocellulose membrane was

incubated in a freshly made 40 ml hybridization buffer containing 20µl of streptavidin-conjugated horseradish peroxide (Roche, Indianapolis, IN) for 45 minutes at room temperature with continuous shaking while completely covered. Afterwards, the nitrocellulose membrane was washed three times in TBS/TWEEN-20, pH 7.5 (5 M NaCl, 0.5 M EDTA, 1 M Tris, pH 7.5, 0.1% Tween) for 5 minutes each at 37°C and incubated in ECL (enhanced chemiluminescent substrate) (Pierce-Thermo Fisher, Rockford, IL) solution for 5 minutes at room temperature. Using a ChemiImager ™ system (AlphaInnotech, San Leandro, CA), the nitrocellulose membrane was visualized and quantified. Results were expressed as the integrated density value (IDV) of the band per microgram of DNA that was loaded on the nitrocellulose membrane.

UDG-Activity Assay:

UDG activity was measured as described by Stuart et al. [23]. A 20µl reaction contained 70 mM HEPES (pH 7.5), 1 mM EDTA, 1 mM DDT, 75 mM NaCl, 0.5% bovine serum albumin (BSA), 90 fmol of 5′-end-labeled single-stranded uracil oligonucleotide and 5µg of nuclear extract. The reaction was incubated for 1 hour at 37°C. Then, the reaction was discontinued by adding 5µg of proteinase K and 1µl of 10% SDS and incubated at 55°C for 30 minutes. DNA was then precipitated in glycogen, ammonium acetate, and ethanol at −20°C overnight. Following precipitation, DNA was resuspended in a loading buffer consisting of 80% formamide, 10 mM EDTA, and 1µg/ml each of bromphenol blue and xylene cyanol FF. The reaction mixture was loaded on a 20% denaturing sequencing gel for separation. Using a Molecular Imager System (Bio-Rad), the glycosylase activity, indicated by the presence of an 11-mer band, was visualized and quantified. The glycosylase activity was determined by calculating the relative amount of the 11-mer oligonucleotide product with the unreacted 30-mer substrate (product/product + substrate). The data was expressed as machine counts per µg of

protein. The reaction mixture and the oligonucleotide without the nuclear extract was the negative control. In order to show that the incision activity was specifically due to UDG and not by another uracil specific glycosylase such as SMUG, 1 unit of uracil DNA glycosylase inhibitor was added to one sample in each reaction.

DNA Base Excision Repair Assay:

A purified 30 base pair oligonucleotide (upper strand, 5′-ATATACCGCGGUCGGCCG ATCAAGCTTATTdd-3′; lower strand, 3′ddTATATGGCGCCGGCCGGCTAGTTC GAATAA-5′) with its ends labeled radioactive and dideoxy ends, contains a G: U mismatch and an HpaII restriction site (CCGG) that is secured by the 3′ amino spacer. The 30 base pair oligonucleotide was incubated with 50 µg of isolated nuclear extract from $ung^{+/+}$ and $ung^{-/-}$ MEFs in a BER reaction mixture (100 mM Tris-HCl (pH 7.5), 5 mM $MgCl_2$, 25 mM DTT, 0.1 mM EDTA, 100 mM ATP, 10 mM NAD, 1 mM dNTPs, 50 mM diTris-phosphocreatine, 10 units/µl of Creatine phosphokinase). The reaction mixtures were incubated for 30 minutes at 37°C and 5 minutes at 95°C in order to end the reaction. The duplex oligonucleotides were then treated with 20 units of HpaII for 1 hour at 37°C in order to determine if the G: U mismatch was repaired to the actual G: C base pair. Electrophoresis with a 20% denaturing gel (19:1 acrylamide: bis-acrylamide gel) was used to separate the duplex oligonucleotides. Repair activity indicated by the presence of a 16-mer-band on the denaturing gel was visualized and then quantified using a Bio-Rad Molecular Imager. The ratio of the 16-mer oligonucleotide product along with the 30-mer substrate (product/substrate) was determined. Data is expressed as machine counts per microgram of protein.

Table 3: Folate assay reaction mixture

Final folate amount (fmol)	0	10	20	40	60	80	100	120
Working buffer	8 µl	8	8	8	8	8	8	8
Folate (2fmol/µl)	---	5 µl	10	20	30	40	50	60
DiH2O	122 µl	117	112	102	92	82	72	62
Media	150 µl	150	150	150	150	150	150	150
L.casei	20 µl	20	20	20	20	20	20	20

Table 4: Folate assay microtiter plate setup

		1	2	3	4	5	6	7	8	9	10	11	12
Folate (fmol)		standard	standard	Standard	blank	sample	s	s	s	s	s	s	s
0	A												
10	B												
20	C												
40	D												
60	E												
80	F												
100	G												
120	H												

Real Time RT-PCR: Once total RNA was isolated from the MEF cells, 2µg of isolated RNA was used to synthesize cDNA using random hexamer primers and an RT-PCR kit (Perkin Elmer, Waltham, MA). The newly synthesized cDNA was then purified using the QIAquick PCR Purification Kit (Qiagen, Valencia, CA). A LightCycler real time PCR machine (Roche, Indianapolis, IN) was used to quantitate the transcripts. Each PCR reaction consisted of 2µL of purified cDNA, 4mM $MgCl_2$, 0.5µM each of sense and antisense primers, and 2µL of FastStart DNA master SYBR Green I enzyme-SYBR reaction mix (Roche). Table 3 details the sequenced primers used. The parameters for all of the amplifications are detailed in Table 3. All the transcripts were normalized to the housekeeping gene, RPL-4.

Table 5: Primer sequences in quantitative real time RT-PCR

Gene	**Sense-primer 5′-3′**	**Anti-sense primer 5′-3′**
UNG	ttcgggaagccgtacttcg	catctgggtccatgtaacac
SMUG	cactggggcctacccatga	ctcccaagcataatccaccg
B-pol (exon 12-13)	agcgagaaggatggaaaggaa	cgtgcgctctcatgttcttat
TDG	gtctgttcatgtcggggctgagtgag	ctgcagtttctgcaccaggatgcgc
MBD4	gatggatccatgggcacgactgggctg	gatctcgaggatgagcttgaaagctgcag
APE1	tagagaattcatgccgaagcgtggga	gcggaagctttcacagtgctaggtat
Ligase3	tgcctgaaaaaggtactgttgg	atgccacaaagtagcgtttga
Housekeeping gene		
Rpl4	ccgtcccctcatatcggtgta	gcatagggctgtctgttgttttt

Table 6: PCR parameters for all amplifications.

	Duration	**Temperature**
Initial denaturing step	10 minutes	99°C
Denature	10 seconds	96°C
Annealing	10 seconds	62°C
Extension	5 seconds	72°C
Melting		40°C-99°C

RESULTS

Doubling time was measured in $UNG^{+/+}$ and $UNG^{-/-}$ mouse embryonic fibroblasts to determine the effect of cell growth in response to folate deficiency. $UNG^{+/+}$ folate depleted significantly increased ($p<0.01$) in doubling time compared to $UNG^{+/+}$ folate added. Similarly, $UNG^{-/-}$ depleted also increased ($p<0.01$) in doubling time compared to $UNG^{-/-}$ folate added. As shown in Figure 1, cell growth is inhibited since doubling time increased in response to folate depletion.

Folate levels in both $UNG^{+/+}$ and $UNG^{-/-}$ folate added and folate depleted mouse embryonic fibroblasts were measured using a *Lactobacillus casei* microbiology assay. The folate added group contained 4 mg/L of folic acid in the media where as the folate-depleted cells consisted of no folate in the media. The $UNG^{+/+}$ folate depleted cells were significantly lower ($p=0.033$) in folate (fmol/cell) compared to $UNG^{+/+}$ folate added group. We observed approximately a 3% reduction in folate in $UNG^{+/+}$ folate depleted cells compared to $UNG^{+/+}$ folate added cells. On the other hand, the $UNG^{-/-}$ cells expressed a higher reduction in folate levels compared $UNG^{+/+}$. Folate levels in $UNG^{-/-}$ folate depleted cells decreased by 10 % compared to the $UNG^{-/-}$ folate added cells. $UNG^{-/-}$ folate depleted was significantly low ($p=0.023$) in folate compared to the $UNG^{-/-}$ folate added group. Such results in Figure 2 as expected, strongly indicate that the absence of folate in growing media induces folate depletion in cells since folate levels in $UNG^{-/-}$ and $UNG^{+/+}$ folate depleted groups were found to be significantly lower.

The aim of this study was to determine uracil accumulation in response to folate deficiency. Previous research has shown that folate deficiency induces uracil misincorporation into DNA (4 million per cell), [2] resulting in double strand breaks and chromosomal

aberrations. The UDG-ASB assay was used to measure uracil levels in $UNG^{-/-}$ and $UNG^{+/+}$ folate added and folate depleted mouse embryonic fibroblasts. As expected and shown in Figure 3, $UNG^{+/+}$ folate depleted group significantly increased ($p<0.01$) in uracil accumulation compared to the $UNG^{+/+}$ folate added. Additionally, $UNG^{-/-}$ folate depleted also exhibited a significant increase ($p<0.01$) in uracil accumulation compared to $UNG^{-/-}$ folate added group. The $UNG^{-/-}$ folate added was also significant with respect to $UNG^{+/+}$ folate added. Similarly, $UNG^{-/-}$ folate deplete was significant with respect to $UNG^{+/+}$ folate depleted. As clearly stated, in Figure 3 and in the provided representative image, uracil accumulation increased significantly in $UNG^{-/-}$ and $UNG^{+/+}$ folate depleted cells. Levels of uracil were much higher in $UNG^{+/+}$ and $UNG^{-/-}$ folate depleted mouse embryonic fibroblasts in comparison to $UNG^{+/+}$ and $UNG^{-/-}$ folate added cells.

Folate deficiency alters the synthesis of thymidylate, which then causes dUMP to accumulate in nucleotide pools. As a result, uracil is misincorporated into DNA. In response, the specific and effective enzyme UDG, excises the uracil from the genome. The removal of uracil by UDG represents the first step in the BER sequential pathway. In response to folate deficiency, we observed a decrease in UDG activity. UDG activity (the presence of an 11-mer band) was visualized in $UNG^{+/+}$ group whereas the $UNG^{-/-}$ group did not exhibit UDG activity since the UNG gene that encodes the enzyme UDG was knocked out from this group. As shown in Figure 4, UDG activity decreased in $UNG^{+/+}$ folate depleted group compared to the control. UDG activity decreased significantly ($p<0.05$) in $UNG^{+/+}$ folate depleted group. This corresponds to a decrease in nuclear UDG protein levels in response to folate deficiency as shown in Figure 6a.

Since BER is a sequential pathway involved in removing folate-induced damage from DNA, BER capacity was measured in response to folate depletion. Repair activity was quantified by calculating percent product over product plus substrate. Previous research has shown BER to

induce DNA damage [23]. Thus, we should expect BER to up-regulated in response to increased levels of DNA damage due to folate deficiency. However, as indicated in Figure 5, BER capacity significantly ($p<0.001$) decreased in response to folate depletion in $UNG^{+/+}$. $UNG^{-/-}$ did not exhibit BER activity since the UNG gene was knocked out from this group sample. Moreover, *β-pol* has been determined to be the rate-limiting step in the BER pathway [20]. Recent studies have shown that the lack of BER induction in response to folate deficiency is followed by a lack of induction in *β-pol* as well.

In order to determine the impact of folate deficiency on BER, the mRNA expression levels of the genes involved in the BER pathway were quantified using real time PCR. All of the BER genes in $UNG^{+/+}$ an $UNG^{-/-}$were normalized to the housekeeping gene RPL-4. The monofunctional glycosylase (Ung) that removes misincorpoarted uracil and oxidized cytosines from DNA, showed a significant decrease ($p<0.05$) in mRNA expression in $UNG^{+/+}$ folate depleted group compared to the folate added $UNG^{+/+}$ cells. As for the $UNG^{-/-}$ cells, Ung was not expressed at all as expected since Ung in this group was knocked out. As for the next enzyme in the BER pathway, APE1 significantly decreased ($p<0.01$) in $UNG^{+/+}$ folate depleted group compared to $UNG^{+/+}$ folate added group. Similarly, APE1 also significantly decreased ($p<0.01$) in $UNG^{-/-}$ folate depleted compared to $UNG^{-/-}$ folate added. As shown in Figure 6a, *β-pol* significantly decreased in $UNG^{+/+}$ folate depleted group compared to $UNG^{+/+}$ folate added group. On the other hand, *β-pol* significantly increased in $UNG^{-/-}$ folate depleted group compared to $UNG^{-/-}$ folate added group. Hence, folate depletion downregulates *β-pol*, in the presence of UNG and upregulates *β-pol* in the absence of UNG. The mRNA expression levels for the scaffolding protein, XRCC-1 that forms a complex with Ligase3 have not yet been measured since the gene has not yet been cloned. However, it is a working progress. As for Ligase3, we observed a

significantly decrease in $UNG^{+/+}$ folate depleted group compared to $UNG^{+/+}$ folate added group. Lgase3 expression also decreased significantly in $UNG^{-/-}$ folate depleted group in comparison with $UNG^{-/-}$ folate added group. Levels of mRNA expression of other uracil DNA glycosylases such as TDG, MDB4, and SMUG were also measured using real time PCR. TDG significantly decreased in folate depleted $UNG^{+/+}$ compared to the control. Additionally, TDG expression was also significantly downregulated in $UNG^{-/-}$ folate depleted group. *Smug* was down regulated in the presence of UNG and down regulated in the absence of UNG in response to folate depletion. Lastly, there was no significant change in MDB4 expression in the presence of UNG in response to folate depletion. However, MBD4 was upregulated in absence of UNG in response to folate depletion. Such results strongly demonstrate that genes involved in the BER pathway were differently regulated during folate deficiency.

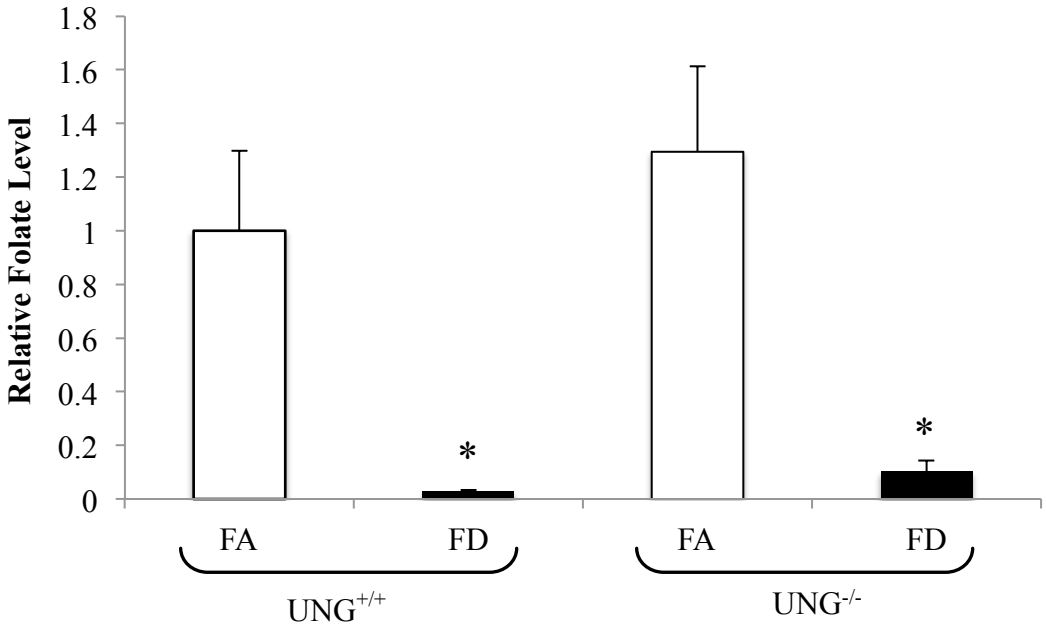

Figure 8: ***Absence of Folate in media induces folate depletion in cells.*** Folate levels in UNG $^{+/+}$ and UNG $^{-/-}$ MEFS was measured using the microbiological assay as described in methods. The level of folate is expressed as fold difference relative to $UNG^{+/+}$/FA. Data is obtained from 4 samples in each group. Folate depletion resulted in greater than 90% reduction in folate in both genotypes. FA=□, FD=■. *p value < 0.01.

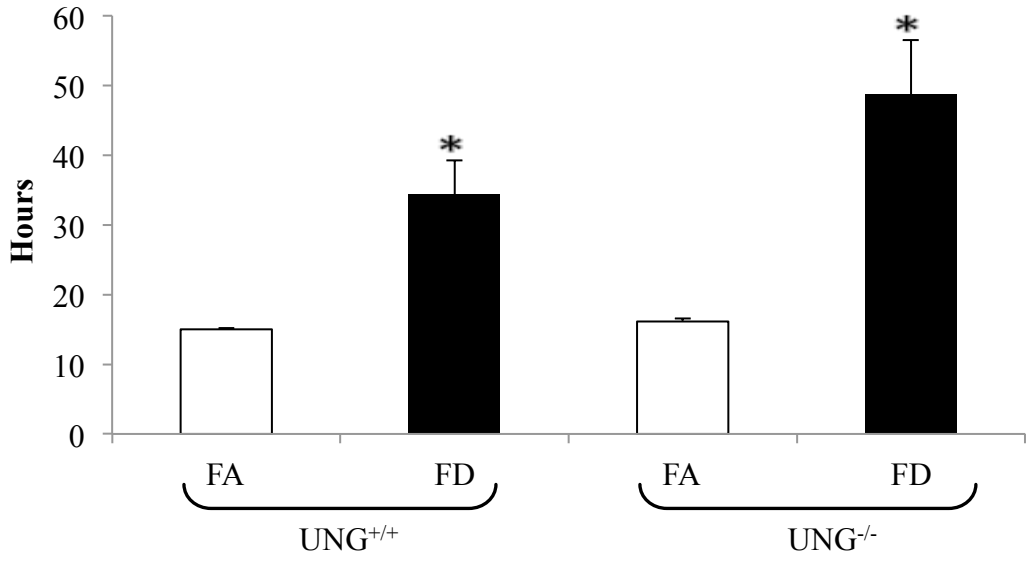

Figure 9: ***Folate depletion inhibits cell growth.*** UNG $^{+/+}$ and UNG $^{-/-}$ decreased in cell growth due to folate depletion. Doubling time was determined as described in methods in UNG $^{+/+}$ and UNG $^{-/-}$ cells. *All values for FD UNG $^{+/+}$ and FD UNG $^{-/-}$ both significantly different from control at $p < 0.01$. FA=□, FD=■.

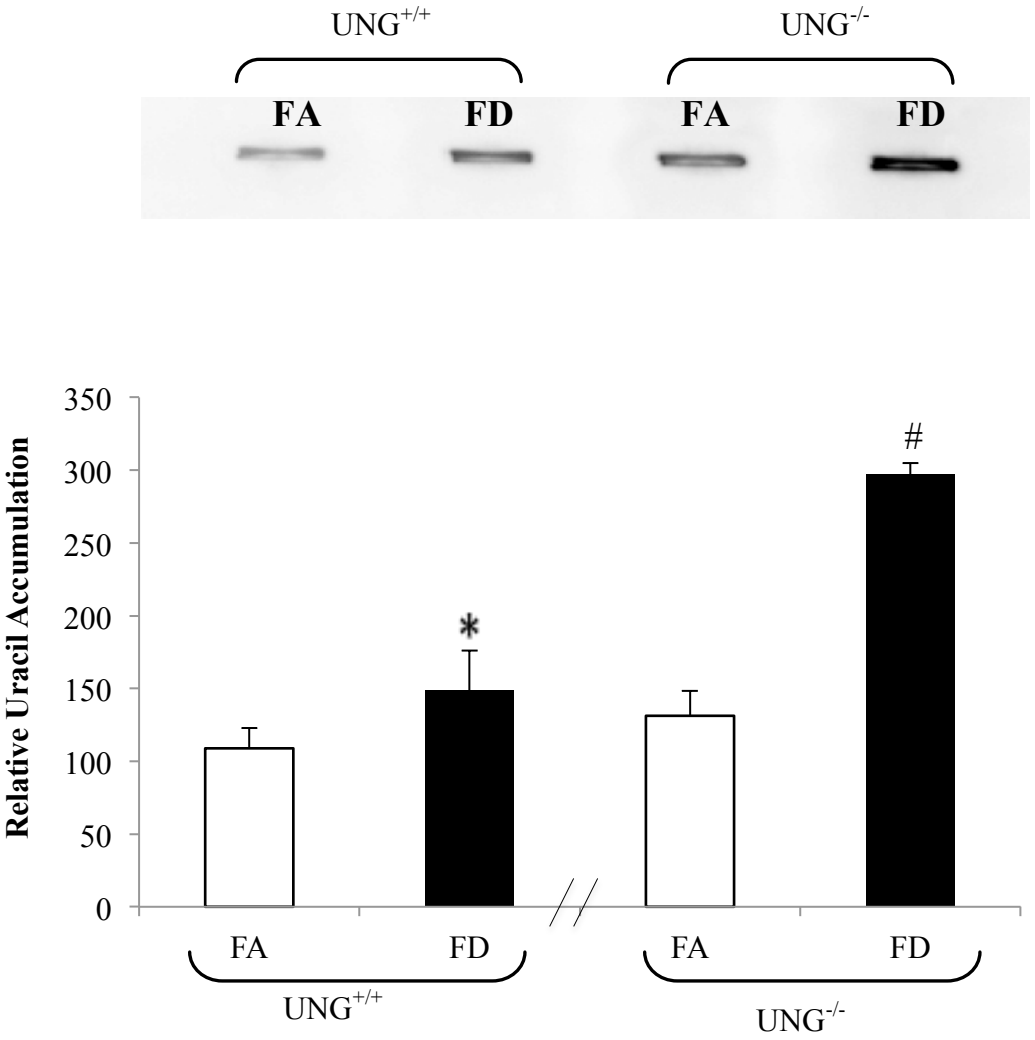

Figure 10: ***UNG deficiency intensifies accumulation of uracil in response to folate depletion.*** Uracil was measured in DNA isolated from folate added and depleted cells with UNG $^{+/+}$ or UNG $^{-/-}$ genotypes as described in methods. Image is a representative sample from both FA and FD of UNG$^{+/+}$ and UNG$^{-/-}$ cells. * $p<0.05$. # $p<0.01$. FA=□, FD=■.

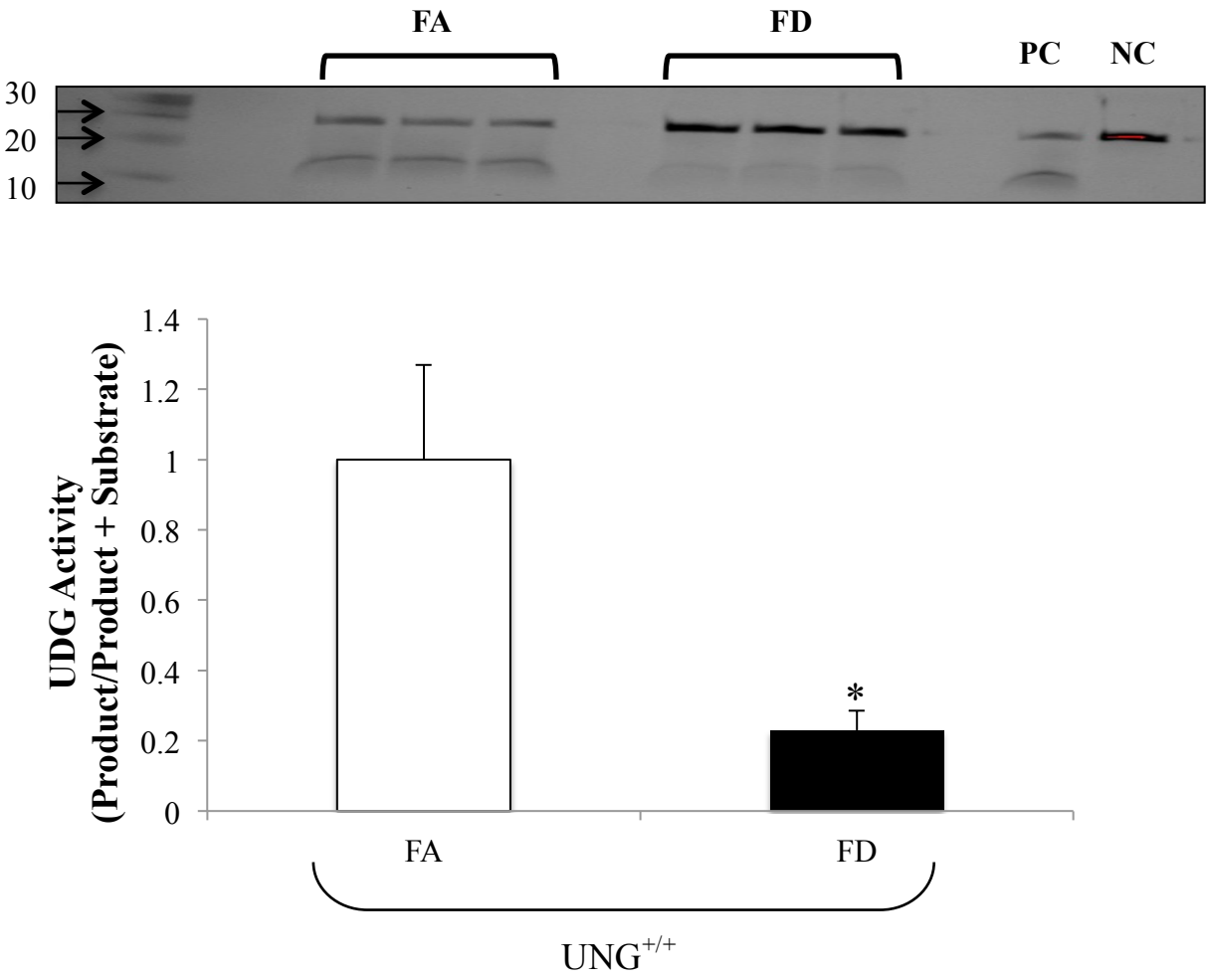

Figure 11: ***Folate depletion significantly reduces Udg activity UNG$^{+/+}$in mouse embryonic fibroblasts.*** UDG activity was measured as described in methods. FA=□, FD=■. *Significantly difference at $p<0.05$

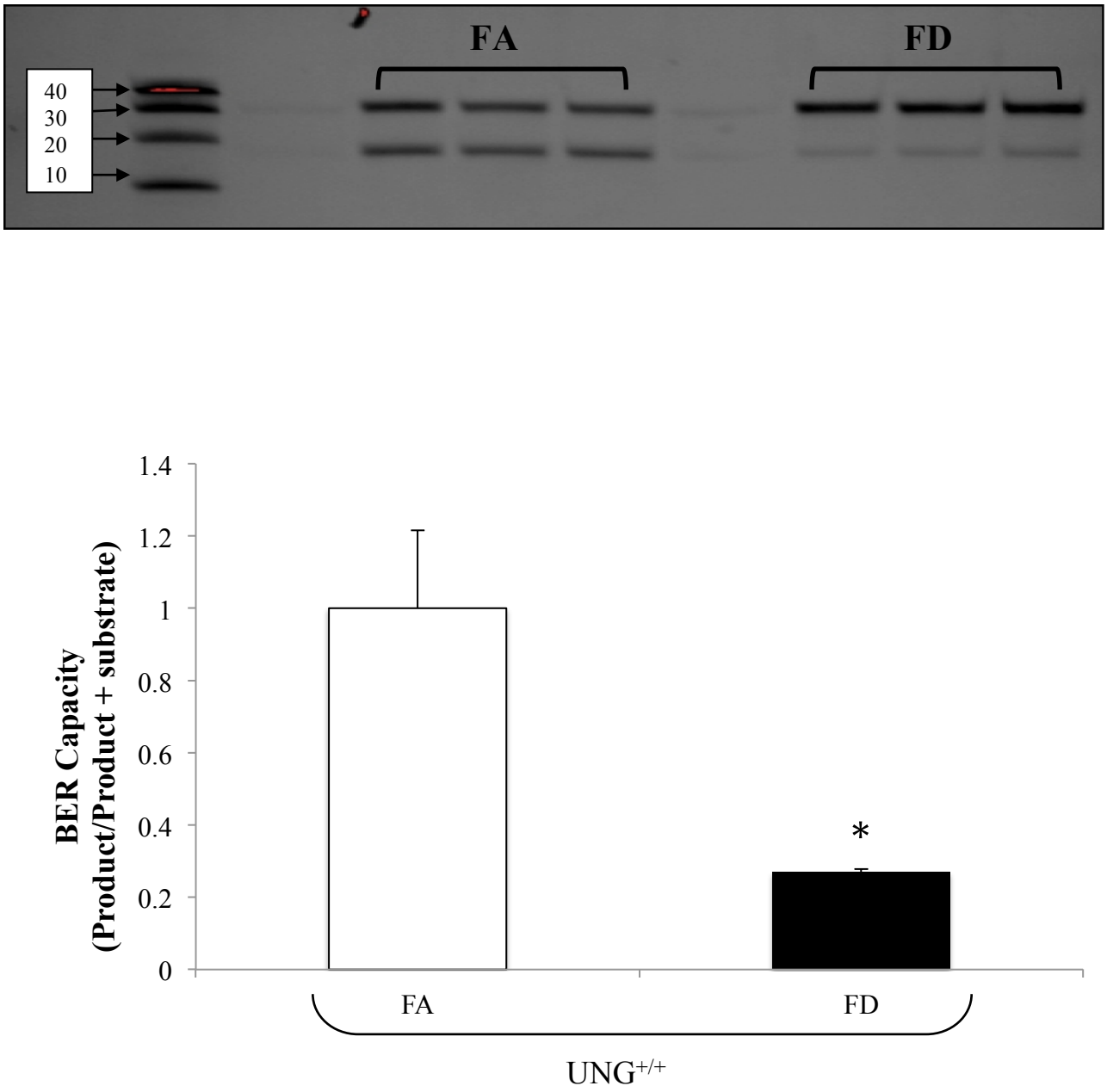

Figure 12: ***Folate depletion inhibits BER capacity in MEF's.*** The in vitro G: U mismatch BER assay was conducted using nuclear extracts obtained from MEFs grown either in folate added or folate depleted media. The reaction products were resolved on a sequencing gel. Repair activity was quantified by calculating percent product over product plus substrate. FA=□, FD=■. Significantly difference at $p<0.001$

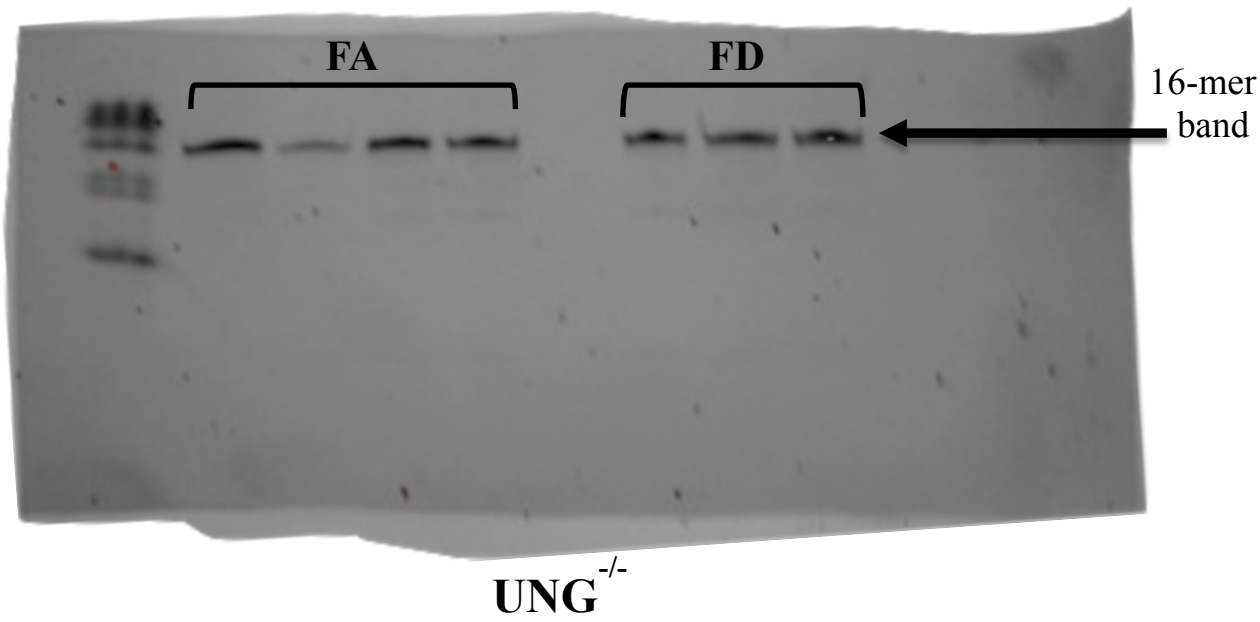

Figure 13: ***Effect of Folate depletion on Base Excision Repair in Ung$^{-/-}$ mouse embryonic fibroblasts***. The in vitro G:U mismatch BER assay was conducted using nuclear extracts obtained from *Ung$^{-/-}$* MEFS grown either in folate added or Folate depleted media. The reaction products were resolved on a sequencing gel. No repair activity was visualized by the appearance of a 16 mer fragment. *Folate added: FA; Folate Depleted: FD.*

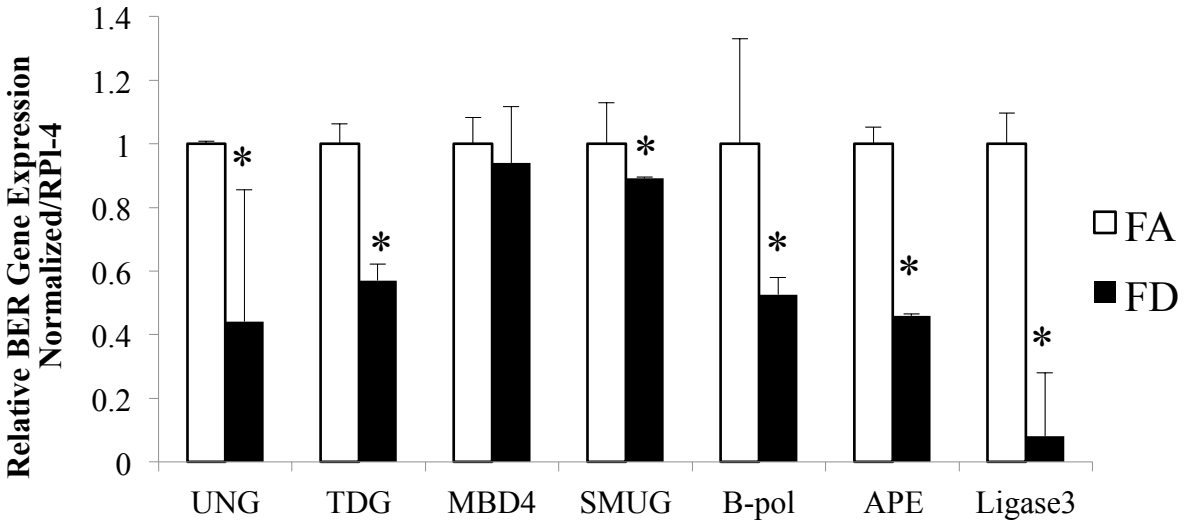

Figure 14: ***Effect of folate deficiency on the expression of uracil-excising enzymes of BER in UNG$^{+/+}$cells.*** mRNA expressions from folate-added and folate-deficient UNG$^{+/+}$ cells. Transcripts were quantified using real-time PCR and normalized to RPL-4. FA=□, FD=■. *Significantly difference at $p<0.05$.

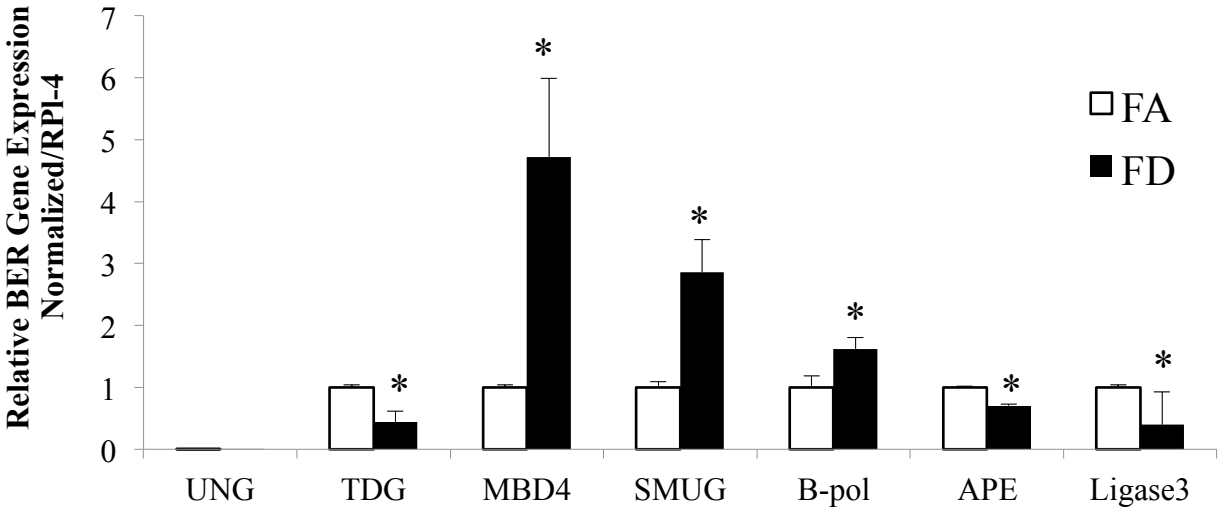

Figure 15: ***Effect of folate deficiency on the expression of uracil-excising enzymes of BER in UNG $^{-/-}$ cells.*** mRNA expressions from folate-added and folate-deficient UNG$^{-/-}$ cells. Transcripts were quantified using real-time PCR and normalized to RPL-4. FA=□, FD=■. *Significantly difference at $p<0.05$.

Discussion

Folate or folic acid is critical in maintaining cell growth in the body, especially during the development of a human embryo. It is necessary in the early development of the spinal cord and the brain to prevent birth neural tube defects (NTDs) and spina bifida [26]. Folate is also essential for the production of DNA that is required for cell growth during the development of fetal organs and tissues in early pregnancy. To determine the effect of cell growth in response to folate deficiency, doubling time was measured in folate depleted UNG $^{+/+}$ and UNG $^{-/-}$ mouse embryonic fibroblasts. We observed a significant increase in doubling time in both folate depleted UNG$^{+/+}$ and UNG$^{-/-}$ mouse embryonic fibroblasts, suggesting that cell growth decreased in response to folate depletion.

Folate levels in folate depleted and folate added UNG $^{+/+}$ and UNG $^{-/-}$ mouse embryonic fibroblasts were measured using the *Lactobacillus casei* microbiological assay to ensure that our folate depleted cells contained no folate. Such assay measures different folic acid derivatives in serum and other biological samples with the use of a 96-well microtiter plate. Our data showed that both UNG $^{+/+}$ and UNG $^{-/-}$ cells significantly decreased in folate in response to folate depletion. Folate depletion resulted in greater than 90% reduction in folate in both genotypes. Such results strongly suggest that folate depletion was induced in our UNG $^{+/+}$ and UNG $^{-/-}$ when folate was absent in our growing media.

Folate has a fundamental role in DNA metabolism [31]. Folate is necessary for the synthesis of dTMP from dUMP. In the absence of folate, the synthesis of thymidylate decreases, creating an imbalance in the deoxyribonucleotide pool. Uracil as a result is misincorporated into DNA during replication and repair [25, 28]. Additionally, uracil is misincorporated into DNA as a result from spontaneous hydrolytic deamination of cytosine. The base excision repair pathway

(BER), initiated by DNA glycosylases, is responsible for the removal of uracil once misincorporated into DNA. However, as these uracil residues are being repaired through BER; there is strong evidence suggesting that single and double strand breaks, chromosome breakage, point mutations, micronucleus formations are generated, increasing the risk of cancer [26, 29]. Additionally, studies have also shown uracil misincorporation into DNA and DNA strand breaks in animal models in response to folate deficiency [31-33].

We hypothesized that levels of uracil would increase in folate depleted $UNG^{+/+}$ and $UNG^{-/-}$ mouse embryonic fibroblasts. Indeed, our hypothesis was proven by our results. Uracil levels significantly increased in UNG $^{-/-}$ folate depleted cells compared to folate added $UNG^{-/-}$ cells. Additionally, uracil levels were also elevated in folate depleted $UNG^{+/+}$ cells compared to the folate added $UNG^{+/+}$ cells. In the absence of folate in both the wildtype and knockout groups, uracil increased significantly. In the *de novo* pathway, dUMP is converted to dTMP by the enzyme thymidylate synthase using the folate co-substrate, N5, N10-methylene THF, as the carbon donor. Without folate, dUMP cannot be converted to dTMP by thymidylate synthase. Hence, dUMP begins to accumulate since it is not capable of being converted to dTMP due to the absence of folate. This mechanism explains as to why we observed high levels of uracil in folate depleted $UNG^{+/+}$ and $UNG^{-/-}$ cells. As the dUMP/dTMP ratio increases in response to folate deficiency, uracil in DNA also increases. As a result, DNA base damage and DNA strand breaks also increase followed by an increase in mtDNA deletions, chromosomal instability, telomere dysfunction, and p53 dysfunction [30].

Uracil DNA glycosylases (UDG) is encoded by the UNG gene [34]. Both UNG1 (mitochondria) and UNG2 (nuclear) are major enzymes responsible enzymes for the removal of uracil in human cells. The removal of uracil by UDG represents the first step in the BER

sequential pathway. The UDG assay was used to determine UDG activity in response to folate depletion in both $UNG^{+/+}$ and $UNG^{-/-}$ mouse embryonic fibroblasts. Majority of UDG activity (the presence of an 11-mer band) is due to the expression of the nuclear isoform UNG2 from the UNG gene locus [35]. We observed a significant decrease in UDG activity in response to folate depletion in $UNG^{+/+}$, suggesting that folate depletion significantly reduces UDG activity. Such decrease in UDG activity is expected to affect BER pathway since BER is the sequential pathway initiated by UDG to repair misincorporated uracil. Corresponding to the UDG activity results, BER activity also significantly decreased in response to folate depletion. Previous research has shown BER to induce DNA damage [23]. Thus, we should expect BER to up-regulated in response to increased levels of DNA damage due to folate deficiency. However, our results show that BER was down regulated in response to folate depletion.

Several genes are involved in the BER pathway that have shown to be affected due to folate depletion. Hence, mRNA expression of UNG, *β-pol,* SMUG, MBD4, TDG, Ligase 3 and APE have been measured in order to determine the affect of folate depletion on the BER pathway. The monofunctional glycosylase, UNG, initiates the BER pathway by removing misincorporated uracil from DNA by cleaving the N-glycosylic bond. Consistent with UDG activity, UNG expression decreased in folate depleted $UNG^{+/+}$ compared to folate added $UNG^{-/-}$. However, as expected, there was no UNG expression in $UNG^{-/-}$ since the gene has been knocked from this group. The second step in BER is catalyzed by APE1, an AP endonuclease, which cleaves the DNA backbone on the 5' side of the AP site. APE 1 expression significantly decreased in folate depleted $UNG^{+/+}$ and $UNG^{-/-}$. As for the rate-limiting step, *β-pol* was down regulated in the presence of UNG in response to folate depletion. However, in the absence of UNG, *β-pol* was upregulated in response to folate depletion. The last enzyme in the BER

pathway, ligase 3, also significantly decreased in gene expression in UNG $^{+/+}$ and UNG $^{-/-}$ in response to folate depletion. Levels of mRNA expression of other uracil DNA glycosylases such as TDG, MDB4, and SMUG were also measured using real time PCR. TDG can remove uracil and 5-bromouracil mispaired with guanine. This enzyme plays an important role in cellular defense against genetic mutation caused by the spontaneous deamination of 5-methylcytosine and cytosine. TDG significantly decreased in folate depleted UNG$^{+/+}$ and was also significantly downregulated in UNG$^{-/-}$ folate depleted group. Smug is a single-strand selective monfunctional uracil DNA glycosylase that removes uracil from single and double stranded DNA in nuclear chromatin. Smug was down regulated in the presence and absence of UNG in response to folate depletion. Lastly, MBD4 acts as a G:T and G:U mismatch specific thymine and uracil glycosylase. Its activity is limited to G: U mismatches and does not move uracil present in single-stranded DNA. There was no significant change in MDB4 expression in the presence of UNG in response to folate depletion. However, MBD4 was upregulated in absence of UNG in response to folate depletion. Such results strongly demonstrate that genes involved in the BER pathway were differently regulated during folate deficiency.

The objective of this research is to determine the impact of folate depletion on uracil accumulation, BER activity and UDG activity in UNG $^{+/+}$ and UNG $^{-/-}$ mouse embryonic fibroblasts (MEFs). Previous studies have shown that folate deficiency results in uracil misincorporation in DNA and therefore increasing genomic instability. Uracil is excised from DNA by the uracil DNA glycosylase (UDG) during the BER pathway. Our results clearly demonstrated that uracil accumulation increased significantly in MEF's in response to folate depletion. Moreover, BER activity and UDG activity also decreased in response to folate depletion while differently regulating the BER genes in the BER pathway.

REFERENCES:

1. Simon KW, Ma H, Dombkowski AA, Cabelof DC: Aging alters folate homeostasis and DNA damage response in colon. *Mech Ageing Dev* 2012, 133(2-3): 75-82.
2. Blount BC, Mack MM, Wehr CM, MacGregor JT, Hiatt RA, Wang G, Wickramasinghe SN, Everson RB, Ames BN: Folate deficiency causes uracil misincorporation into human DNA and chromosome breakage: implications for cancer and neuronal damage. *Proc Natl Acad Sci U S A* 1997, 94(7): 3290-3295.
3. Cabelof DC, Raffoul JJ, Nakamura J, Kapoor D, Abdalla H, Heydari AR: Imbalanced base excision repair in response to folate deficiency is accelerated by polymerase beta haploinsufficiency. *J Biol Chem* 2004, 279(35): 36504-36513.
4. Herbert V: Vitamin B-12 and folic acid supplementation. *Am J Clin Nutr* 1997, 66(6): 1479-1480.
5. Herbert V. Folic Acid. In: Shils M, Olson J, Shike M, Ross AC, ed. *Nutrtion in Health and Disease*. Baltimore: William & Wilkins, 1999.
6. U.S. Department of Agriculture, Agriculture Research Service. 2003. USDA National Database for Standard Reference, Release 16. Nutrition Data Laboratory Home page, http://www.nal.usda.gov/fnic/cig-bin/nut_search.pl
7. Oakley GP, Jr., Adams MJ, Dickinson CM: More folic acid for everyone, now. *J Nutr* 1996, 126(3): 751S-755S.
8. Daly S, Mills JL, Molloy AM, Conley M, Lee YJ, Kirke PN, Weir DG, Scott JM: Minimum effective dose of folic acid for food fortification to prevent neural-tube defects. *Lancet* 1997, 350(9092): 1666-1669.
9. Ames BN, Wakimoto P: Are vitamin and mineral deficiencies a major cancer risk? *Nat Rev Cancer* 2002, 2(9): 694-704.
10. Gropper, Sareen, A. S, Jack L. Smith, and James L. Groff. Advanced Nutrition and Human Metabolism. Australia: Wadsworth/Cengage Learning, 2009. Print.
11. Stover PJ: One-carbon metabolism-genome interactions in folate-associated pathologies. *J Nutr* 2009, 139(12): 2402-2405.
12. Gregory JF, 3rd: Case study: folate bioavailability. *J Nutr* 2001, 131(4 Suppl): 1376S-1382S.

13. Institute of Medicine. Food and Nutrition Board. Dietary Reference Intakes: Thiamin, riboflavin, niacin, vitamin B6, folate, vitamin B12, pantothenic acid, biotin, and choline. National Academy Press. Washington, DC, 1998.
14. Lamprecht SA, Lipkin M: Chemoprevention of colon cancer by calcium, vitamin D and folate: molecular mechanisms. *Nat Rev Cancer* 2003, 3(8): 601-614.
15. Duthie SJ, Narayanan S, Sharp L, Little J, Basten G, Powers H: Folate, DNA stability and colo-rectal neoplasia. *Proc Nutr Soc* 2004, 63(4): 571-578.
16. Duthie SJ: Folic acid deficiency and cancer: mechanisms of DNA instability. *Br Med Bull* 1999, 55(3): 578-592.
17. Berger SH, Pittman DL, Wyatt MD: Uracil in DNA: consequences for carcinogenesis and chemotherapy. *Biochem Pharmacol* 2008, 76(6): 697-706.
18. Cabelof DC, Raffoul JJ, Yanamadala S, Ganir C, Guo Z, Heydari AR: Attenuation of DNA polymerase beta-dependent base excision repair and increased DMS-induced mutagenicity in aged mice. *Mutat Res* 2002, 500(1-2): 1 35-145
19. Scott JM, Weir DG. The methyl folate trap. A physiological response in man to prevent methyl group deficiency in kwashiorkor (methionine deficiency) and an explanation for folic-acid induced exacerbation of subacute combined degeneration in pernicious anaemia. Lancet. 1981 Aug 15; 2(8242):337-40.
20. Cabelof DC, Raffoul JJ, Yanamadala S, Guo Z, Heydari AR: Induction of DNA polymerase beta-dependent base excision repair in response to oxidative stress in vivo. *Carcinogenesis* 2002, 23:1419-1425**.**
21. Srivastava DK, Berg BJ, Prasad R, Molina JT, Beard WA, Tomkinson AE, Wilson SH: Mammalian abasic site base excision repair. Identification of the reaction sequence and rate-determining steps. *J Biol Chem* 1998, 273:21203-21209.
22. Endres M, Biniszkiewicz D, Sobol RW, Harms C, Ahmadi M, Lipski A, Katchanov J, Mergenthaler P, Dirnagl U, Wilson SH, et al: Increased postischemic brain injury in mice deficient in uracil-DNA glycosylase. *J Clin Invest* 2004, **113:**1711-1721.
23. Stuart JA, Karahalil B, Hogue BA, Souza-Pinto NC, Bohr VA: Mitochondrial and nuclear DNA base excision repair are affected differently by caloric restriction. *FASEB J* 2004, 18:595-597.

24. Cabelof DC, Nakamura J, Heydari AR: A sensitive biochemical assay for the detection of uracil. *Environ Mol Mutagen* 2006, 47:31-37.
25. Home DW, Patterson D: Lactobacillucsasei Microbiological Assay of Folic Acid Derivatives in 96-Well Microtiter Plate. *Clinical Chemistry* 1988, 34:11-2357.
26. Bailey LB: New standard for dietary folate intake in pregnant women. *Am J Clin Nutr* 2000, 71:1304S-1307S
27. Hazra A, Selhub J, Chao WH, Ueland PM, Hunter DJ, Baron JA: Uracil misincorporation into DNA and folic acid supplementation. *Am J Clin Nutr* 2010, 91:160-165.
28. Elliott B, Jasin M: Double-strand breaks and translocations in cancer. *Cell Mol Life Sci* 2002, 59:373-385
29. C. Wagner, Biochemical role of folate in cellular metabolism, in: L.B. Bailey (Ed.), Folate in Health and Disease, Marcel Dekker Inc. Publ., 1995, pp. 23–42.
30. I. Eto, C.L. Krumdieck, Role of vitamin B-12 and folate deficiencies in carcino- genesis, in: L.A. Poirier, P.M. Newberne, M.W. Pariza (Eds.), Essential Nutrients in Carcinogenesis, Plenum Press Publ., 1986, pp. 313–331.
31. B.C. Blount, B.N. Ames, DNA damage in folate deficiency, Bailleres Clin. Haematol. 8 (3) (1995) 461–478.
32. Folate (vitamin B9) and vitamin B12 and their function in the maintenance of nuclear and mitochondrial genome integrity FIND
33. Duthie SJ, Grant G, Narayanan S: Increased uracil misincorporation in lymphocytes from folate-deficient rats. *Br J Cancer* 2000, 83:1532-1537.
34. Kim YI, Shirwadkar S, Choi SW, Puchyr M, Wang Y, Mason JB: Effects of dietary folate on DNA strand breaks within mutation-prone exons of the p53 gene in rat colon. *Gastroenterology* 2000, 119(1):151-161
35. Pogribny IP, Muskhelishvili L, Miller BJ, James SJ: Presence and consequence of uracil in preneoplastic DNA from folate/methyl-deficient rats. Carcinogenesis 1997, 18(11): 2071-2076.
36. Akbari M, Otterlei M, Pena-Diaz J, Krokan HE: Different organization of base excision repair of uracil in DNA in nuclei and mitochondria and selective upregulation of mitochondrial uracil-DNA glycosylase after oxidative stress. *Neuroscience* 2007, 145**:**1201-1212.

37. Krokan HE, Drablos F, Slupphaug G: Uracil in DNA--occurrence, consequences and repair. *Oncogene* 2002, 21(58): 8935-8948.

ABSTRACT

URACIL ACCUMULATION IN FOLATE DEPLETED MOUSE EMBRYONIC FIBROBLASTS

by

ENEIDA DOKO

MAY 2012

Advisor: Dr. Diane Cabelof

Major: Nutrition and Food Science

Degree: Master of Science

Folate is a water-soluble vitamin B that plays a critical co-enzyme in the *de novo* nucleotide synthesis and other biochemical processes including DNA metabolism, DNA repair, DNA methylation, and cellular growth. Folate deficiency has been associated to increase the risk of neural tube defects (NTDs) and cancers of the lung, breast, colon, cervix, esposphagus and brain. Most importantly, folate deficiency has been shown to increase uracil misincorporation into DNA and therefore induce DNA damage repaired by the base excision repair (BER) pathway. In response to folate depletion, levels of thmidylate decrease in the deoxyribonucelotide pool, resulting in uracil being misincorporated into DNA instead of thymine during replication and repair. Uracil misincorporation into DNA is believed to be the biological mechanism of how folate affects carcinogenesis. We evaluated the impact of folate depletion on uracil accumulation, BER activity and UDG activity in folate depleted $UNG^{+/+}$ and $UNG^{-/-}$ mouse embryonic fibroblasts (MEFs). Additionally, cell growth in response to folate deficiency was also determined by completing doubling time in folate depleted $UNG^{+/+}$ and $UNG^{-/-}$ cells. As expected, levels of uracil significantly increased in $UNG^{+/+}$ and $UNG^{-/-}$ cells in response to folate depletion. Uracil-DNA glycosylase (Udg) activity, which is responsible for the

removal of uracil during the base excision (BER) pathway, significantly decreased in folate depleted $UNG^{-/-}$ cells. Such decreases in Udg activity corresponded to the decrease in nuclear UDG protein levels in response to folate deficiency. Similarly, BER capacity significantly ($p<0.001$) decreased in response to folate depletion in $UNG^{+/+}$ cells, suggesting that folate deficiency inhibits BER in mouse embryonic fibroblasts.

AUTOBIOGRAPHICAL STATEMENT

MCPHS in Worcester Massachusetts College of Pharmacy Accelerated 3-year program	2012-2015
Wayne State University Masters of Sciences Nutrition and Food Sciences	(2009-2012) Detroit, MI
Wayne State University BS in Liberal Arts & Sciences Nutrition and Food Sciences	(2005-2009) Detroit, MI
OSHA Laboratory Safety Training Certificate	(May 2011)
CITI Program Wayne State University Nutrition Dept. **(**Certificate to conduct research studies)	(2008 –2010)
FASEB Journal During Senior Year at WSU Name published for conducting research in a Freshmen Health Study at WSU	(2008-2009)
Oakwood Healthcare System in Dearborn Nutrition Department Volunteer in the Nutrition Department	(2009 – 2010)
TSS Substitute Teacher Substitute teacher for downriver district	(2011-Present)